Supplementary Material

Biosynthesis of Orthogonal Molecules Using Ferredoxin and Ferredoxin-NADP$^+$ Reductase Systems Enables Genetically Encoded PhyB Optogenetics

Phillip Kyriakakis[1,#], Marianne Catanho[1,#], Nicole Hoffner[3], Walter Thavarajah[1], Vincent Jian-Yu[1] Hu, Syh-Shiuan Chao[4], Athena Hsu[5], Vivian Pham[6], Ladan Naghavian[1], Lara E. Dozier[2], Gentry Patrick[2] and Todd P. Coleman[1]

Affiliation and Correspondence

[1] Department of Bioengineering, University of California, San Diego, 9500 Gilman Drive, San Diego, La Jolla, California, 92093-0412, USA

[2] Section of Neurobiology, Division of Biological Sciences, University of California San Diego, La Jolla, California 92093-0347

[3] Neurosciences Graduate Program, University of California, San Diego, 9500 Gilman Drive, La Jolla, CA 92093, United States

[4] Frank H. Better School of Medicine, Quinnipiac University, 370 Bassett Rd, North Haven, CT 06473, USA

[5] School of Medicine, University of California, San Diego, 9500 Gilman Drive, San Diego, La Jolla, California, 92093, USA

[6] University of Iowa, Roy J. and Lucille A. Carver College of Medicine 451 Newton Road Iowa City, IA, USA 52242

[#] These authors contributed equally to this work.

Correspondence and requests for materials should be addressed to P.K. or T.P.C. (email: pkyriaka@ucsd.edu or tpcoleman@ucsd.edu).

Illumination Circuits and Software.

To obtain programmable control needed to drive the high-power LEDs used in our experiments, we designed the light control system shown in **Figure S5**. Using this system, we have precise timing and light-intensity control for 8 experimental boxes that required red and/or far-red illumination. Each black box can house a standard 6-well, 12-well, 24-well, 96-well plate or can be fitted for a single dish with minimum modifications. The system can be replicated for experiments requiring a larger number of boxes or experimental conditions. Far-red and red lights can be controlled independently if placed in the same box. For our experimental setup, boxes contained either far-red 735nm LEDs or red 660nm LEDs. The light control system employs: (a) an Arduino Uno and voltage regulation circuits, managed through a (b) user interface developed in LabVIEW (National Instruments).

The voltage regulation circuit is shown in **Figure S6**. Coupled with the Arduino signals, this system delivers light pulses with precise timing and intensity control to the experiment boxes. The circuit is build using a LM317T linear voltage regulator (STMicroelectronics), a NPN general-purpose amplifier (2N2222, Fairchild Semiconductors), a resistor and a trimmer potentiometer (Helitrim, model 75PK10K). An external power supply was outfitted for the circuit (Safety Mark, 12V 1.5A Switch-mode power supply). The power supply allows the circuit to vary its current and voltage needs depending upon the intensity chosen by a user using the trimmer potentiometer.

The LabVIEW user interface, available for download at https://github.com/mcatanho/Kyriakakis_et_al_SupplementaryFiles (See Supplementary Note), controls the Arduino and connected circuits. It allows the user to connect to the Arduino effortlessly and to control experimental conditions such as time delay before illumination, a total duration of sample illumination, and pulse frequencies for each individual illumination box. It also contains digital displays of all relevant experimental times (**Figure S5**).

Kinetic Model Development and Parametrization.

We demonstrate the biochemical interactions among the enzymes shown in **Figure 1A** in the production of PCB through a kinetic model developed with the PySB framework [1]. The model's code, equations, and simulation files are available for download at https://github.com/mcatanho/Kyriakakis_et_al_SupplementaryFiles (See Supplementary Note). The quantitative mathematical model was parametrized (**Table S5**) by experimental data and uses ordinary differential equations to describe the changes in the concentration of the molecular components of the reaction.

For the model, we assume that the production of PCB can be described by the set of sequential steps shown in **Table S4**, and depicted in **Figure 1A**. This kinetic model builds upon Tu *et al*. description of the four electron reduction of biliverdin IX-alpha (BV) to phycocyanobilin (PCB), catalyzed by cyanobacterial phycocyanobilin:ferredoxin oxidoreductase (PcyA) [2]. As demonstrated experimentally in this work, the ferredoxin (Fd) and ferredoxin:oxidoreductase (FNR) complex is of paramount importance to the redox metabolism in plants and cyanobacteria, working as an electron transfer complex to reduce or oxidize enzymes in different pathways, further acting to reduce or NADP+ to NADPH or the reverse of this reaction [3–5]. As described in **Figure 1A**, the first step in the PCB production pathway involves the formation of the HO1:Heme complex, which receives electron transfers from reduced ferredoxin (Fd_{red}), producing BV [6]. Following a PcyA:BV complex is formed, which in turn also receives electron transfers from Fd_{red}, leading to the production of PCB. As the preferred electron donor for HO1 and PcyA, reduced Fd allows for continuous turnover of those enzymes in the PCB production pathway [6].

The reactions described above to produce PCB are shown in **Scheme 1.** The model assumes that those molecules are present *in vitro* at stoichiometry levels compatible with our transient transfection plasmid ratio. For simplicity, the model ignores differences in overall expression and degradation of each enzyme. Our model does not assume degradation of heme or BV, since we assumed there were saturating amounts in the cell medium. We also assume

that the oxidized ferredoxin, a result of the electron transfer to the HO1:Heme and PcyA:BV complexes, is renewed in the $NADP^+$/NADPH pathway catalyzed by FNR. We probed the proposed model directly as proposed in literature [2,7,8], and similar pathways published. We complement this work showing the model's agreement with the hypothesized pathway, confirming that in the presence of heme, Fd and FNR are the rate limiting factors to produce PCB, confirmed experimentally in **Figure 1B.** We also show in **Figure S7A**, how PCB's production dependence on Heme and the NADP/NAPDH pathway, characterized by the presence of Fd and FNR, are interlinked.

Design and Parametrization of the Mathematical Model.

Coupled, first order, ordinary differential equations (ODEs), parametrization of the model was performed using previously reported endogenous PCB production curves [8]. The reaction schemes below were translated into the PySB rule-based language. Rates were calculated through a parametric sweep method utilizing maximum-likelihood minimization for model-fitting procedures. The rule-based model simulates PCB production, following the reactions described in the **Scheme 1** below.

Scheme 1

(1) Formation of the Heme and HO1 complex

(2) Formation of Fd_{red}:HO1:Heme complex, electron transfer from Fd_{red}, producing BV

(3) Formation of the BV:PcyA complex

(4) Fd_{red}:PcyA:BV complex formation, and electron transfer from Fd_{red}, producing PCB

(5) FNR-enabled Fd reduction

(6) Spontaneous degradation of PCB, as described by Mueller *et al* [8].

$$Heme + HO1 \underset{k_2}{\overset{k_1}{\rightleftarrows}} HO1{:}\,Heme \quad (1)$$

$$HO1{:}\,Heme + Fd_{red} \underset{k_4}{\overset{k_3}{\rightleftarrows}} Fd_{red}{:}\,HO1{:}\,Heme \quad (2)$$

$$Fd_{red}{:}\,HO1{:}\,Heme \xrightarrow{k_5} HO1{:}\,BV + Fd_{oxi} \quad (3)$$

$$HO1{:}\,BV \xrightarrow{k_6} BV + HO1 \quad (4)$$

$$BV + PcyA \underset{k_8}{\overset{k_7}{\rightleftarrows}} PcyA{:}\,BV \quad (5)$$

$$PcyA{:}\,BV + Fd_{red} \underset{k_{10}}{\overset{k_9}{\rightleftarrows}} Fd_{red}{:}\,PcyA{:}\,BV \quad (6)$$

$$Fd_{red}{:}\,PcyA{:}\,BV \xrightarrow{k_{11}} PcyA{:}\,PCB + Fd_{oxi} \quad (7)$$

$$PcyA{:}\,PCB \xrightarrow{k_{12}} PCB + PcyA \quad (8)$$

$$Fd_{oxi} \xrightarrow{k_{13}} Fd_{red} \quad (9)$$

$$PCB \xrightarrow{k_{deg,PCB}} \emptyset \quad (10)$$

The set of coupled ordinary differential equations obtained from those reactions, following mass-action kinetics [9], is shown in **Scheme 2**.

Scheme 2

$$\frac{d[Heme](t)}{dt} = -k_1[Heme][HO1] + k_2[HO1{:}\,Heme] \quad (1)$$

$$\frac{d[HO1](t)}{dt} = -k_1[Heme][HO1] + k_2[HO1{:}\,Heme] + k_6[HO1{:}\,BV] \quad (2)$$

$$\frac{d[Fd_{red}](t)}{dt} = -k_9[PcyA{:}BV][Fd_{red}] + k_{10}[Fd_{red}{:}PcyA{:}BV] - k_3[Fd_{red}][HO1{:}Heme] + k_{13}[Fd_{oxi}] + k_4[Fd_{red}{:}HO1{:}Heme] \quad (3)$$

$$\frac{d[Fd_{oxi}](t)}{dt} = k_{11}[Fd_{red}{:}PcyA{:}BV] - k_{13}[Fd_{red}] + k_5[Fd_{red}{:}HO1{:}Heme] \quad (4)$$

$$\frac{d[PcyA](t)}{dt} = k_8[PcyA{:}BV] + k_{12}[PcyA{:}PCB] - k_7[PcyA][BV] \quad (5)$$

$$\frac{d[Heme{:}HO1](t)}{dt} = k_1[Heme][HO1] - k_3[Fd_{red}][HO1{:}Heme] - k_2[HO1{:}Heme] + k_4[Fd_{red}{:}HO1{:}Heme] \quad (5)$$

$$\frac{d[Fd_{red}{:}HO1{:}Heme](t)}{dt} = k_3[Fd_{red}][HO1{:}Heme] - (k_4 + k_5)[Fd_{red}{:}HO1{:}Heme] \quad (6)$$

$$\frac{d[HO1{:}BV](t)}{dt} = k_5[Fd_{red}{:}HO1{:}Heme] - k_6[HO1{:}BV] \quad (7)$$

$$\frac{d[BV](t)}{dt} = -k_7[Pcya][BV] + k_6[HO1{:}BV] + k_8[PcyA{:}BV] \quad (8)$$

$$\frac{d[PcyA{:}BV](t)}{dt} = -k_9[PCyA{:}BV][Fd_{red}] - k_8[PcyA{:}BV] + k_{10}[Fd_{red}{:}BV{:}PcyA] + k_7[BV][PcyA] \quad (9)$$

$$\frac{d[Fd_{red}{:}PcyA{:}BV](t)}{dt} = k_9[Fd_{red}][PcyA{:}BV] - (k_{10} + k_{11})\,[Fd_{red}{:}PcyA{:}BV] \quad (10)$$

$$\frac{d[PcyA{:}PCB](t)}{dt} = -k_{12}[PcyA{:}PCB] + k_{11}\,[Fd_{red}{:}PcyA{:}BV] \quad (11)$$

$$\frac{d[PCB](t)}{dt} = k_{12} * [PcyA{:}PCB] - k_{degPCB} * [PCB] \quad (12)$$

1.1.1. Fitting the Model to Experimental Data.

The model's unknown parameters were determined by a maximum likelihood approach fitted to the data shown in Muller *et al* [8]. Units are defined in S.I. units with concentrations as the number

of molecules for species ($\#molecules$, or c), and parameters as bimolecular rate constants in $\#molecules/s^{-1}$(or c/s^{-1}).

Sum-of-Squares and Parameter Estimation

We assume that the system of ordinary differential equations (ODE) shown in **Scheme 2** can be represented as a dynamical system given by an N-dimensional state variable $\boldsymbol{x}(t) \in \mathbb{R}^N$, at time $t \in I = [t_0, t_f]$, which is the unique and differentiable solution for the initial value problem given by:

$$\dot{\boldsymbol{x}}(t) = f(\boldsymbol{x}(t), t, \boldsymbol{\theta}) \qquad \boldsymbol{x}(t_0) = \boldsymbol{x_0}$$

As such, the ODE depends on certain parameters $\boldsymbol{\theta} \in \mathbb{R}^{n_p}$ [10]. Also, let Y_i denote the data of measurement $i = 1, \ldots, n$, where n represents the total amount of data. Moreover, the data Y_i satisfies $Y_i = g(t_i, \boldsymbol{\theta}) + \sigma_i \epsilon_i$, for some function $\boldsymbol{g}: \mathbb{R}^d \rightarrow \mathbb{R}^{obs}$, and $d \geq obs, \sigma_i > 0$ and ϵ_i are independent and standard Gaussian distributed random variables [10]. The function $\boldsymbol{g}(\cdot)$ is continuously differentiable. To estimate the parameters $\boldsymbol{\theta}$, given the initial conditions, utilizing the principle of maximum-likelihood to yield a cost function to be minimized gives us:

$$\mathcal{L}(\boldsymbol{\theta}) = \sum_{i=1}^{n} \frac{\left(Y_i - g(\boldsymbol{x}(t_i; \boldsymbol{\theta}), \boldsymbol{\theta})\right)^2}{2\sigma_i^2}$$

We perform a direct minimization of $\mathcal{L}$ with respect to $\boldsymbol{\theta}$ to obtain the parameters show in **Table S5**, and used throughout the experiments described next.

Implementation of Experiments.

Our model was used to gain insight into the dependencies of this pathway and to further validate our experimental results. HO1 and PcyA were assumed to be at equimolar amounts and Fd at

1/10th of that molar concentration. Unless stated otherwise, the following initial conditions were used. If not listed, the initial concentrations were set to zero at t=0.

[Heme](0) = 100

[HO1](0) = 10

[$Fd_{red,oxi}$](0) = 5

[PcyA](0) = 10

Experiment 1: Fd and Heme dependence

We determined experimentally the rate limiting factors are Fd, followed by Fd+FNR and finally heme. To model this experimental result, we performed a sweep over initial concentrations of Fd ([Fd](0)), heme ([Heme](0)), and rate of renewal of Fd by FNR (k_{13}). The result of those sweeps are shown in **Figure S7A** (Heme concentration vs. Fd renewal) and **Figure S7B** (Heme concentration vs. Fd concentration). The resulting graphs show the dependency of PCB production on those molecules, and how the initial condition of each affects the rate of production of PCB.

Experiment 2: 2E vs 4E.

Our experimental results show that PCB is only produced to high levels under the presence of Fd, PcyA, and HO1. To model this experimental result, we modified the following parameters to simulate the lack of compatible Fd, namely a “two enzyme” (2E) case, that limits the production of PCB versus the output of the pathway when all four enzymes (4E) are present. For the 2E case, we set [$Fd_{red,oxi}$](0) to zero (**Figure S8A**).

Experiment 3: Species Specificity as Demonstrated by Different Binding Coefficients.

To demonstrate how the species specificity between Fd and HO1/PcyA plays a pivotal role in the amount of PCB produced, we performed a decreasing sweep through the parameters k_3 and k_9,

which control binding of HO1 and PcyA to Fd respectively. The sweeps were started at the parameter's value as described in **Table S5** to 1e-3 c/s^{-1}. The resulting graph is shown in **Figure S8B**.

Experiment 4: Variable Levels of Heme.

In this experiment, we performed a sweep over a range of Heme concentrations, from 100, 10, 5, 1 and 0.1 c. This experiment, similar to **Figure** S7, shows the heme dependency of PCB production. The respective graph is shown in **Figure S8C**.

SUPPLEMENTARY TABLES

Table S1. Similarity Tables for Ferredoxin and Ferredoxin-dependent Bilin Reductases.

A

Ferredoxin-dependent Bilin Reductases		
	THEEB-PCYA	Syn-PCYA
W/SS		
ARATH-Hy2		
% Identity	14.454	8.627
Identical AA	49	49
Similar AA	82	89
W/O SS		
ARATH-Hy2		
% Identity	15.667	15.282
Identical AA	47	46
Similar AA	80	88

B

With Signal Sequence				
	THEEB	SYNP2	ADX_HUMAN	FDX2_HUMAN
THEEB				
% Identity	100	71.429	10.811	12.973
Identical AA	98	70	20	24
Similar AA	0	16	37	36
SYNP2				
% Identity	71.429	100	11.17	12.5
Identical AA	70	97	21	23
Similar AA	16	0	37	32
FER1_ARATH				
% Identity	39.597	42.568	16.754	19.565
Identical AA	59	63	32	36
Similar AA	26	23	55	47
FER2_ARATH*				
% Identity	39.597	44.595	17.617	17.857
Identical AA	59	66	34	35
Similar AA	26	20	44	46
FER3_ARATH				
% Identity	40.645	40.645	18.135	17.949
Identical AA	63	63	35	35
Similar AA	25	23	57	49
FER4_ARATH				
% Identity	32.432	40.645	15.426	12.821
Identical AA	48	63	29	25
Similar AA	31	23	57	53
MFDX1_ARATH				
% Identity	12.563	12.183	31.25	32.258
Identical AA	25	24	65	70
Similar AA	37	35	58	56
MFDX2_ARATH				
% Identity	13.568	9.645	30.653	34.653
Identical AA	27	19	61	70
Similar AA	37	40	65	63
ADRX_YEAST				
% Identity	15.517	16.000	29.798	33.333
Identical AA	27	28	59	61
Similar AA	31	28	52	56
ADX_HUMAN				
% Identity	10.811	11.170	100	30.688
Identical AA	20	21	184	58
Similar AA	37	37	0	61
FDX2_HUMAN				
% Identity	12.973	12.500	30.688	100
Identical AA	24	23	58	183
Similar AA	36	32	61	0

C

Without Signal Sequence				
	THEEB	SYNP2	ADX_HUMAN	FDX2_HUMAN
THEEB				
% Identity	100	71.429	16.000	18.045
Identical AA	98	70	20	24
Similar AA	0	16	37	35
SYNP2				
% Identity	71.429	100	16.406	15.909
Identical AA	70	97	21	21
Similar AA	16	0	37	35
FER1_ARATH				
% Identity	59.184	63.918	16.8	18.321
Identical AA	58	62	21	24
Similar AA	25	22	37	31
FER2_ARATH*				
% Identity	59.184	67.010	16.126	18.321
Identical AA	58	65	20	24
Similar AA	26	20	34	31
FER3_ARATH				
% Identity	59.434	59.434	16.794	21.053
Identical AA	63	63	22	28
Similar AA	25	23	36	32
FER4_ARATH				
% Identity	48.485	49.495	15.152	13.74
Identical AA	48	49	20	18
Similar AA	31	29	41	37
MFDX1_ARATH				
% Identity	15.244	14.815	32.927	38.272
Identical AA	25	24	54	62
Similar AA	37	35	39	43
MFDX2_ARATH				
% Identity	21.600	15.447	43.2	45.455
Identical AA	27	19	54	60
Similar AA	37	40	38	38
ADRX_YEAST				
% Identity	23.077	22.881	38.71	36.641
Identical AA	27	27	48	48
Similar AA	31	29	35	39
ADX_HUMAN				
% Identity	16.000	16.406	100	31.579
Identical AA	20	21	124	42
Similar AA	37	37	0	46
FDX2_HUMAN				
% Identity	18.045	15.909	31.579	100
Identical AA	24	21	42	131
Similar AA	35	35	46	0

(A) The similarity of ferredoxin-dependent bilin reductases and similarity of Fds. **(B)** The similarity of ferredoxins with eukaryotic sequences containing signal sequences. **(C)** The similarity of ferredoxins with eukaryotic sequences with signal sequences removed. Sequence alignments were done using UniProt (http://www.uniprot.org/).
Fd types: ■ Cyanobacterial; ■ Chloroplastic; ■ Mitochondrial.
Species: ■ Cyanobacterial, ■ Arabidopsis; ■ Yeast; ■ Human.

Table S2. Plasmids Used in This Study.

Genes for enzymes were synthesized by Genscript and Integrated DNA Technologies. Plasmids and sequences will be made available on Addgene or upon request.

Plasmid Number	Description	Source	Addgene Plasmid ID
pMZ-802	FLuc under control of pTet (tetO13-CMVmin-FLuc-pA)	Müller et al.	N/A
pPKm-102	pcDNA3 - mOrange	This study	90493
pPKm-105	pcDNA3 - PhyB NT - GBD,	This study	104853
pPKm-112	pcDNA3 - MTAD - PIF3,	This study	90494
pPKm-113	pcDNA3 - MTAD - PIF6,	This study	90495
pPKm-118	pcDNA3 - 5X UAS - pFR Luciferase	This study	90491
pPKm-145	Empty plasmid, pSIN-EF1-alpha-IRES-puro	This study	90505
pPKm-163	pcDNA3 - PIF3 - GBD,	This study	104854
pPKm-195	pcDNA3 - PhyB NT - MTAD	This study	90496
pPKm-196	pcDNA3 - PIF6-DBD	This study	90511
pPKm-202	pcDNA3 – CMVmin 5X UAS - pFR - Luciferase	This study	90492
pPKm-226	pcDNA3 - PIF3 – VPR	This study	90497
pPKm-227	pcDNA3 - VPR - PIF3	This study	90498

pPKm-230	pSIN - EF1-alpha - PIF3 - MTAD - IRES - PhyB - GBD	This study	90499
pPKm-231	pSIN - EF1-alpha - MTS - tFd - P2A - MTS - tFNR, encoding for mitochondrial-tagged *Thermosynechococcus elongatus* Ferredoxin (Fd) and Ferredoxin-NADP(+) oxi0doreductase (FNR)	This study	90500
pPKm-232	pSIN - EF1-alpha - MTS tHO1 - P2A - MTS - tPCYA, encoding for mitochondrial-tagged *Thermosynechococcus elongatus* Heme Oxygenase-1 (HO1) and phycocyanobilin:ferredoxin oxidoreductase (PcyA)	This study	90501
pPKm-233	pSIN - EF1-alpha - sFD - P2A - MTS - sFNR, encoding for *Synechococcus sp.* Ferredoxin (Fd) and Ferredoxin-oxidoreductase (FNR)	This study	90508
pPKm-234	pSIN - EF1-alpha - MTS sHO1 - P2A - MTS - sPCYA, encoding for mitochondrial-tagged *Synechococcus sp.* Heme Oxygenase (HO1) and phycocyanobilin:ferredoxin oxidoreductase (PcyA),	This study	90507
pPKm-235	pSIN - EF-1alpha - MTS sHO1 - P2A - MTS - sPCYA,	This study	90509

	encoding for mitochondrial-tagged *Synechococcus sp.* Heme Oxygenase-1 (HO1) and *Arabidopsis thaliana* phytochromobilin:ferredoxin oxidoreductase (Hy2) replacing the chloroplastic targeting sequence with a MTS		
pPKm-240	pSIN - EF1-alpha cyto-sHO1-P2A – cyto-sPcyA, encoding for cytoplasmic-tagged *Synechococcus sp* HO1 and PcyA	This study	90510
pPKm-241	pSIN - EF1-alpha - cyto-sFd - P2A - cyto-sFNR, vector encoding for cytoplasmic-tagged *Synechococcus sp* Fd and FNR	This study	104855
pPKm-243	pSIN - EF1-alpha - mOrange-P2A-mitosfGFP, mOrange and mitochondrial-tagged sfGFP	This study	90506
pPKm-244	pSIN – EF1-alpha - MTS - tHO1 - P2A - MTS - tPCYA - IRES - MTS - tFD - P2A - MTS - tFNR	This study	90502
pPKm-245	pSIN - EF1-alpha - MTS - tHO1 - P2A - MTS - tPCYA - P2A - MTS - tFD - P2A - MTS - tFNR	This study	90503
pPKm-248	pSIN - EF1-alpha - MTS - tPCYA - IRES - MTS - tHO1 -	This study	90504

	P2A - MTS - tFD - P2A - MTS - tFNR		
pPKm-292	pcDNA3 – GAL4_DNA BD - MTAD	This study	105816
pPKm-293	pcDNA3 – TET DNA BD - MTAD	This study	105817
pPKm-300	pSIN - EF1-alpha - MTS - tFd, encoding for mitochondrial-tagged *Thermosynechococcus elongatus* Ferredoxin (Fd)	This study	104626
pRL-TK	Control reporter for constitutive expression of wildtype Renilla luciferase (Rluc) under pRL-TK	Promega	E2241

Table S3. Transfection and Illumination Details for each Figure.

Figure 1B	HEK293 cells were transfected 24 hours after plating. Calculations are for each well. Transfected in a 6 well plate. Cells were harvested 44 hours post-transfection followed by Immunoprecipitation and Zn-PAGE as described in methods.	
NE control		
Plasmid	**DNA mass (ng)**	**DNA Ratio**
pPKm-105	125	1/20
pPKm-102	125	1/20
pPKm-145	1125	18/20
M2-sPcyA		
Plasmid	**DNA mass (ng)**	**DNA Ratio**
pPKm-105	125	1/20
pPKm-243	125	1/20
pPKm-234	1125	9/20
pPKm-145	1125	9/20
M4-sPcyA		
Plasmid	**DNA mass (ng)**	**DNA Ratio**
pPKm-105	125	1/20
pPKm-243	125	1/20
pPKm-234	1125	9/20
pPKm-233	1125	9/20
M2-tPcyA		
Plasmid	**DNA mass (ng)**	**DNA Ratio**
pPKm-105	125	1/20
pPKm-243	125	1/20

	pPKm-232	1125	9/20
	pPKm-145	1125	9/20

M4-tPcyA

Plasmid	DNA mass (ng)	DNA Ratio
pPKm-105	125	1/20
pPKm-243	125	1/20
pPKm-232	1125	9/20
pPKm-231	1125	9/20

M2-Hy2

Plasmid	DNA mass (ng)	DNA Ratio
pPKm-105	125	1/20
pPKm-243	125	1/20
pPKm-235	1125	9/20
pPKm-145	1125	9/20

M4-Hy2

Plasmid	DNA mass (ng)	DNA Ratio
pPKm-105	125	1/20
pPKm-243	125	1/20
pPKm-235	1125	9/20
pPKm-233	1125	9/20

Figure 2A

HEK293 cells were transfected 24 hours after plating. Calculations are for each well. Transfected two of each in a 6 well plate, one with and one without heme. 10µM (Frontier scientific) was added 18 hours and 43 hours post-transfection. Cells were harvested 44 hours post transfection followed by Immunoprecipitation and Zn-PAGE as described in methods.

NE control

Plasmid	DNA mass (ng)	DNA Ratio
pPKm-105	125	1/20
pPKm-243	125	1/20
pPKm-145	1125	18/20

C2

Plasmid	DNA mass (ng)	DNA Ratio
pPKm-105	125	1/20
pPKm-243	125	1/20
pPKm-240	1125	9/20
pPKm-145	1125	9/20

C4

Plasmid	DNA mass (ng)	DNA Ratio
pPKm-105	125	1/20
pPKm-243	125	1/20
pPKm-240	1125	9/20
pPKm-241	1125	9/20

M2

Plasmid	DNA mass (ng)	DNA Ratio
pPKm-105	125	1/20
pPKm-243	125	1/20
pPKm-234	1125	9/20
pPKm-145	1125	9/20

M4

Plasmid	DNA mass (ng)	DNA Ratio
pPKm-105	125	1/20

pPKm-243	125	1/20
pPKm-234	1125	9/20
pPKm-233	1125	9/20

Figure 2B HEK293 cells were transfected 24 hours after plating. Calculations are for each well in a 6-well plate. Cells were harvested 44 hours post transfection followed by Immunoprecipitation and Zn-PAGE as described in methods.

M2

Plasmid	DNA mass (ng)	DNA ratio
pPKm-105	125	1/20
pPKm-243	125	1/20
pPKm-232	1125	9/20
pPKm-145	1125	9/20

M3

Plasmid	DNA mass (ng)	DNA ratio
pPKm-105	125	1/20
pPKm-243	125	1/20
pPKm-232	1125	9/20
pPKm-300	1125	9/20

M4

Plasmid	DNA mass (ng)	DNA ratio
pPKm-105	125	1/20
pPKm-243	125	1/20
pPKm-232	1125	9/20
pPKm-231	1125	9/20

NE

Plasmid	DNA mass (ng)	DNA ratio
pPKm-105	125	1/20
pPKm-243	125	1/20
pPKm-145	2250	18/20

Figure 3D

HEK293 cells were transfected 24h after plating, followed by a medium change 24h after transfection. For illumination, 1µmol/m2/s 1-minute pulses of red light were delivered for 24h, starting 12h after the medium change. Cells were kept in darkness before and after illumination. Lysis was performed 72h after transfection, and samples stored in -20C until assayed.

9HP:9EV (1:1 ratio HP:EV)

Plasmid	DNA mass (ng)	DNA ratio
pPKm-102	425.0	25.5/30
pPKm-105	16.7	1/30
pPKm-112	16.7	1/30
pPKm-232	16.7	1/30
pPKm-202	16.7	1/30
pRL-TK	8.3	0.5/30

9HP:9FF (1:1 ratio HP:FF)

Plasmid	DNA mass (ng)	DNA ratio
pPKm-102	408.3	24.5/30
pPKm-105	16.7	1/30
pPKm-112	16.7	1/30
pPKm-232	16.7	1/30
pPKm-231	16.7	1/30
pPKm-202	16.7	1/30

	pRL-TK	8.3	0.5/30

	Plasmid	DNA mass (ng)	DNA ratio
17HP:1EV (17:1 ratio HP:EV)	pPKm-102	158.3	9.5/30
	pPKm-105	16.7	1/30
	pPKm-112	16.7	1/30
	pPKm-232	283.3	17/30
	pPKm-202	16.7	1/30
	pRL-TK	8.3	0.5/30

	Plasmid	DNA mass (ng)	DNA ratio
17HP:1FF (17:1 ratio HP:FF)	pPKm-102	141.7	8.5/30
	pPKm-105	16.7	1/30
	pPKm-112	16.7	1/30
	pPKm-232	283.3	17/30
	pPKm-231	16.7	1/30
	pPKm-202	16.7	1/30
	pRL-TK	8.3	0.5/30

Figure 3F

HEK293 Cells were transfected 24h after plating, followed by a medium change 24h after transfection. For illumination, 1 µmol/m^2/s 1-minute pulses of red light were delivered for 24h, starting 12h after the medium change. Cells were kept in darkness before and after illumination. Cell lysis was performed 72h after transfection, and samples stored in -20C until assayed.

245

Plasmid	DNA mass (ng)	DNA ratio

pPKm-102	10	1/50
pPKm-230	225	22.5/50
pPKm-245	225	22.5/50
pPKm-202	20	2/50
pRL-TK	20	2/50

244

Plasmid	DNA mass (ng)	DNA ratio
pPKm-102	10	1/50
pPKm-230	225	22.5/50
pPKm-244	225	22.5/50
pPKm-202	20	2/50
pRL-TK	20	2/50

248

Plasmid	DNA mass (ng)	DNA ratio
pPKm-102	10	1/50
pPKm-230	225	22.5/50
pPKm-248	225	22.5/50
pPKm-202	20	2/50
pRL-TK	20	2/50

Figure 4, Figure 5

Cells were transfected 24h after plating, followed by a medium change 24h after transfection. In Figure 4D, red light at 1µmol/m^2/s, 0.1µmol/m^2/s, 0.01 µmol/m^2/s and 0.001 µmol/m^2/s were delivered for a total of 24 hours. Similarly, in Figure 4E, continuous illumination for 24h was delivered to the cells, in the intensities listed above. For Figure 4F, red light at 0.1 and 1µmol/m^2/s was continuously delivered or shone for 1-minute pulses every

4 minutes, 9 minutes or 29 minutes, starting 12h after medium change for a total of 24h. For Figures 4G, red light at the intensity of 1µmol/m^2/s was delivered to the cells every 30minutes, every hour, every 2 hours, every 4 hours, 6 hours, 8 hours or every 12 hours. For Figure 5B, cells were kept in darkness, illuminated with far-red light, red light for 24 hours, or with 12 hours or red light followed by darkness or far-red light. For Figure 5C, cells were illuminated with red light at 1 µmol/m^2/s and given a 1 min red light pulse every 5 minutes for 24 hours. In all cases, cells were kept in darkness before and after illumination. Far-red samples were kept under constant illumination starting at medium change. Cell lysis was performed 72h after transfection, and samples stored in -20C until assayed.

All conditions

Plasmid	DNA mass (ng)	DNA ratio
pPKm-102	10	1/50
pPKm-230	225	22.5/50
pPKm-248	225	22.5/50
pPKm-202	20	2/50
pRL-TK	20	2/50

Supplementary Figure 1

HEK293 Cells were transfected 24h after plating on polylysine-coated coverslips. 43 hours later media was changed with media+5µM PCB (Frontier Scientific P14137) added to the NE+PCB control. One hour later cells were rinsed in PBS and fixed in 4%Paraformaldehyde for 10 minutes. Next cells were incubated in permeabilization buffer (5% BSA + 0.3% TritonX-100 in PBS) for 30min, followed by primary antibodies overnight at 4°C in antibody buffer (2% BSA + 0.2% TritonX-100 in PBS; anti-flag mouse monoclonal 1:1000 (Sigma F3165) anti-HA rabbit polyclonal 1:500 (Santa Cruz Y-11)); Next coverslips were rinsed twice and washed three time in PBS and then incubated in antibody buffer with goat anti-mouse AlexaFluor 488 1:1000 (Thermo-Fisher A11001) goat anti-rabbit AlexaFluor 568 1:1000 (Thermo-Fisher A11011)). Coverslips were then mounted with Fluoromount-G (SouthernBiotech 0100-20). Images were taken using a DeltaVision RT Deconvolution Microscope.

NE control

Plasmid	DNA mass (ng)	DNA Ratio
pPKm-105	100	4/20
pPKm-145	400	16/20

C2

Plasmid	DNA mass (ng)	DNA Ratio
pPKm-105	100	4/20
pPKm-240	375	15/20
pPKm-145	25	1/20

C4

Plasmid	DNA mass (ng)	DNA Ratio
pPKm-105	100	4/20

	pPKm-240	375	15/20
	pPKm-241	25	1/20

M2

Plasmid	DNA mass (ng)	DNA Ratio
pPKm-105	100	4/20
pPKm-234	375	15/20
pPKm-145	25	1/20

M4

Plasmid	DNA mass (ng)	DNA Ratio
pPKm-105	100	4/20
pPKm-234	375	15/20
pPKm-233	25	1/20

Figure S2C

HEK293 cells were transfected 24 hours after plating. For this experiment, 15uM of PCB (Frontier Scientific) was added 47h after transfection. Light at 10 μmol/m^2/s was delivered 1h after PCB was added, and cells were illuminated for 1 minute every 4 minutes for 24 hours. 24h after illumination, cells were lysed and stored at -20C until assay.

P6-DBD

Plasmid	DNA mass (ng)	DNA Ratio
pPKm-102	1579	12/19
pPKm-196	263	2/19
pPKm-195	263	2/19
pPKm-118	263	2/19
pRL-TK	132	1/19

Plasmid	DNA mass (ng)	DNA Ratio

P3-DBD

pPKm-102	1579	12/19
pPKm-163	263	2/19
pPKm-195	263	2/19
pPKm-118	263	2/19
pRL-TK	132	1/19

P6-AD

Plasmid	DNA mass (ng)	DNA Ratio
pPKm-102	1579	12/19
pPKm-105	263	2/19
pPKm-113	263	2/19
pPKm-118	263	2/19
pRL-TK	132	1/19

P3-AD

Plasmid	DNA mass (ng)	DNA Ratio
pPKm-102	1579	12/19
pPKm-105	263	2/19
pPKm-112	263	2/19
pPKm-118	263	2/19
pRL-TK	132	1/19

Figure S3C

HEK293 cells were transfected 24h after plating, followed by a medium change 24h after transfection. For this experiment, 15uM of PCB (Frontier Scientific) was added 47h after transfection. Light at 1 μmol/m^2/s in 1-minute pulses of red light was delivered 1h after PCB was added. Cells were kept in darkness before and after illumination. Lysis was performed 72h after transfection, and samples stored in -20C until assayed.

P3-MTAD

Plasmid	DNA mass (ng)	DNA ratio
pPKm-102	325	33/50
pPKm-105	50	5/50
pPKm-112	50	5/50
pPKm-118	50	5/50
pRL-TK	25	2/50

P3-VPR

Plasmid	DNA mass (ng)	DNA ratio
pPKm-102	325	33/50
pPKm-105	50	5/50
pPKm- 226	50	5/50
pPKm-118	50	5/50
pRL-TK	25	2/50

VPR-P3

Plasmid	DNA mass (ng)	DNA ratio
pPKm-102	325	33/50
pPKm-105	50	5/50
pPKm- 227	50	5/50
pPKm-118	50	5/50
pRL-TK	25	2/50

Figure S4A HEK293 cells were transfected 24h after plating, followed by a medium change 24h after transfection. Cells were lysed 72h after transfection, and samples stored in -20C until assayed.

Renilla

Plasmid	DNA mass (ng)	DNA ratio
pPKm-102	480	48/50
pRL-TK	20	2/50

TET-UAS-CMVmin

Plasmid	DNA mass (ng)	DNA ratio
pPKm-102	430	43/50
pMZ-802	50	5/50
pRL-TK	20	2/50

G4-UAS-Flucmin

Plasmid	DNA mass (ng)	DNA ratio
pPKm-102	430	43/50
pPKm-118	50	5/50
pRL-TK	20	2/50

G4-UAS-CMVmin

Plasmid	DNA mass (ng)	DNA ratio
pPKm-102	430	43/50
pPKm-202	50	5/50
pRL-TK	20	2/50

Figure S4B

HEK293 cells were transfected 24h after plating, followed by a medium change 24h after transfection. Cells were lysed 72h after transfection, and samples stored in -20C until assayed.

TET-CMV

(pMZ-802)

Plasmid	DNA mass (ng)	DNA ratio
pPKm-102	380	38/50
pPKm-293	50	5/50
pMZ-802	50	5/50
pRL-TK	20	2/50

G4-CMV

(pPKm-202)

Plasmid	DNA mass (ng)	DNA ratio
pPKm-102	380	38/50
pPKm-292	50	5/50
pPKm-202	50	5/50
pRL-TK	20	2/50

Table S4. Parameters for the Model.

Parameter	Value	Description
k1	0.1228	HO1 and heme binding rate
k2	1e-12	HO1 and heme unbinding rate
k3	0.5687	HO1:Heme and Fd_{red} binding rate
k4	1e-12	HO1:Heme:Fd_{red} unbinding rate
k5	0.2285	Fd_{red}:HO1:Heme unbinding, forming HO1:BV and Fd_{oxi}
k6	0.4750	HO1 unbinding from BV, releasing BV
k7	0.1825	Rate of BV and PcyA binding, forming PcyA:BV
k8	1e-12	PcyA:BV unbinding rate
k9	0.2500	PcyA:BV and Fd_{red} binding rate, forming Fd_{red}:PcyA:BV
k10	1e-12	Unbinding rate of Fd_{red}:PcyA:BV
k11	0.1220	Fd_{red}:PcyA:BV unbinding, forming PcyA:PCB and Fd_{oxi}
k12	0.2667	Unbinding of PcyA:PCB, producing PCB
k13	0.2250	Reduction of Fd_{oxi}, forming Fd_{red}
$k_{deg,PCB}$	0.1567	Degradation of PCB
Heme, at t=0	100	Initial concentration of Heme
HO-1, at t=0	10	Initial concentration of HO-1
PcyA, at t=0	10	Initial concentration of PcyA
$Fd_{red,oxi}$, at t=0	5	Initial concentration of Fd (red and oxi)

c: arbitrary unit of concentration.

Unless indicated otherwise, all other concentrations were considered to be zero.

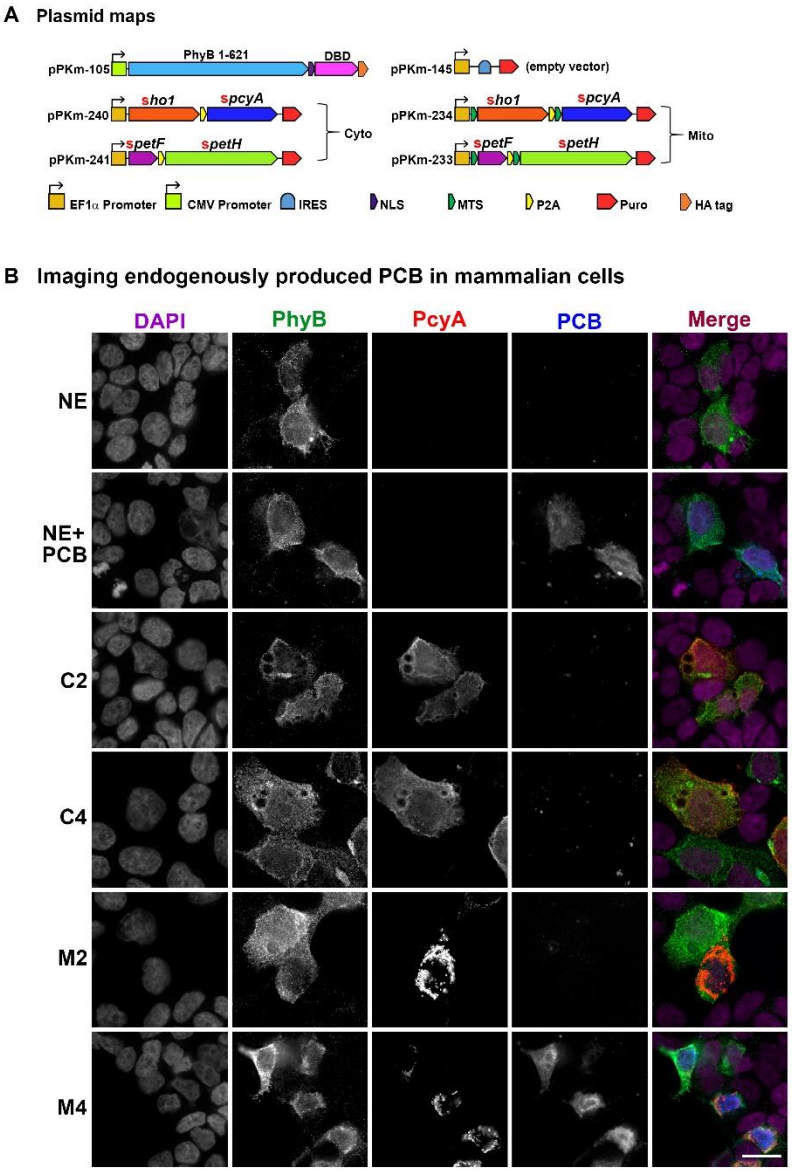

Figure S1. Imaging endogenously produced PCB in mammalian cells. HEK293 cells were transfected with PhyB alone (NE), *PhyB*+5μM PCB (NE+PCB), cytoplasmic *sho1*+*spcyA* (C2), cytoplasmic *sho1*+*spcyA*+*spetF*+*spetH* (C4), mitochondrial *sho1*+*spcyA* (M2), or mitochondrial *sho1*+*spcyA*+*spetF*+*spetH* (M4). DAPI DNA stain was imaged using the DAPI channel (purple). PhyB tagged with HA was imaged using anti-HA (green), PcyA tagged with FLAG was imaged using anti-FLAG (red). PCB was imaged using the Cy-5 channel (blue). All images were taken under the same exposure and contrast settings using a 60X (1.40NA) objective.

IRES = Internal Ribosome Entry Site, NLS = Nuclear Localization Sequence, MTS = Mitochondria Targeting Sequence, P2A = 2A self-cleaving peptide, DBD = DNA Binding Domain, R/FR = Red light/Far-red light.

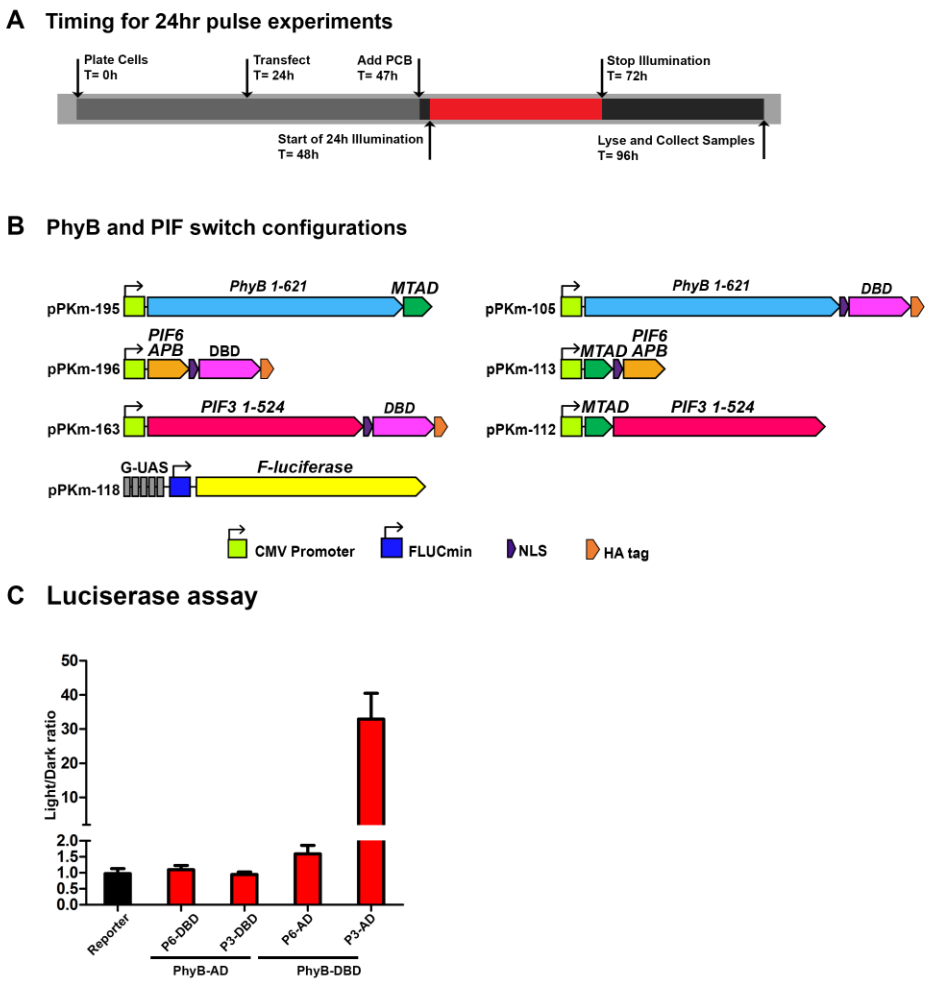

Figure S2: Optimizing PhyB and PIF light switches for mammalian cells. **(A)** HEK293 cells were transfected, illuminated and incubated in 15µM PCB as shown in the timeline. **(B)** Plasmid maps of the different PhyB and PIF designs. **(C)** Comparison of gene activation using several variations of PhyB-PIF light switchable promoters. The negative control consists of UAS luciferase plasmid alone. In the first two experimental conditions, PIF6 or PIF3 are fused to the DBD (P6-DBD and P3-DBD, respectively) and PhyB is fused to the AD (PhyB-AD). The second two experimental conditions contain PhyB fused to the DBD along with PIF6 and PIF3 fused to the AD (P6-AD and PIF3-AD, respectively). Fold gene expression was calculated comparing cells in red light to cells in darkness, after normalizing to a Renilla control (n=6).

DBD = DNA Binding Domain, AD = Activation Domain

(Error bars = s.d. (***) = $p<0.001$, Statistics were calculated using one-way ANOVA with Bonferroni post-test using GraphPad Prism 5.01).

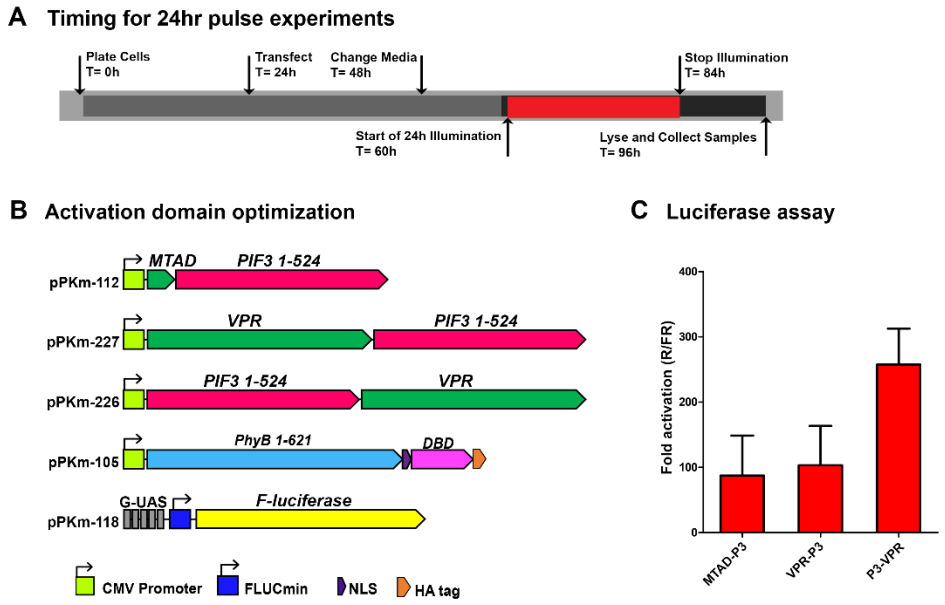

Figure S3: Optimizing PhyB and PIF gene switch. **(A)** Timeline for experiments where HEK293 cells were transfected and illuminated for 24 hours. **(B)** Plasmid maps for constructs with MTAD and VPR activation domains fused to the C-terminal or N-terminal of PIF3 **(C)** Comparison of MTAD and VPR fusions with PIF3 effects of luciferase gene activation. Fold gene expression was calculated comparing cells incubated in red light to cells incubated in far-red light, after normalizing to a Renilla control (n=3).

DBD = DNA Binding Domain, AD = Activation Domain, MTAD = Minimal Trans-Activation Domain, VPR = VP64+P65+RTA, R/FR = Red light/Far-red light

(Error bars = s.d. (***) = $p<0.001$, Statistics were calculated using one-way ANOVA with Bonferroni post-test using GraphPad Prism 5.01).

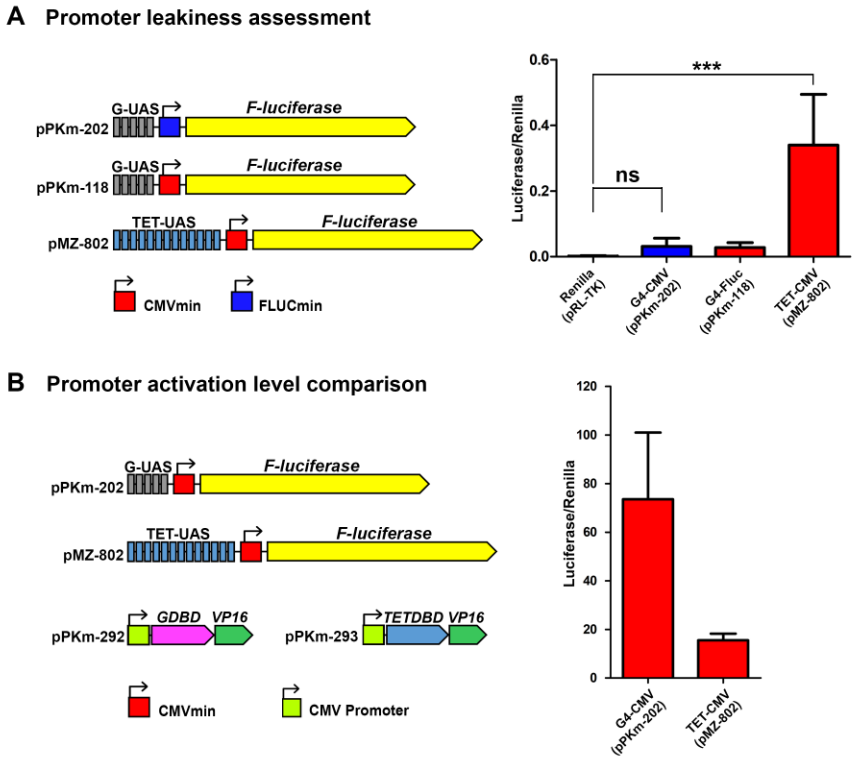

Figure S4: Comparing reporter constructs. **(A)** Leakiness analysis comparing different reporter vectors. HEK293 cells were transfected using the reporter vector along with Renilla (pRL-TK) alone or with Renilla+filler DNA (pRL-TK +pPKm-102) plasmids. Leaky luciferase values were compared to Renilla alone (n=5) **(B)** Activation level comparison of Gal4 UAS and TET UAS reporters. HEK293 cells transfected with pPKm-202 or pMZ-802 along with pPKm-292 or pPKm-293 respectively (n=3).

G-UAS = Gal4 UAS, TET-UAS = TET UAS, GDBD = Gal4 DNA Binding Domain, TETDBD = TET DNA Binding Domain. (Error bars = s.d. (***) = $p<0.001$, Statistics were calculated using one-way ANOVA with Bonferroni post-test using GraphPad Prism 5.01).

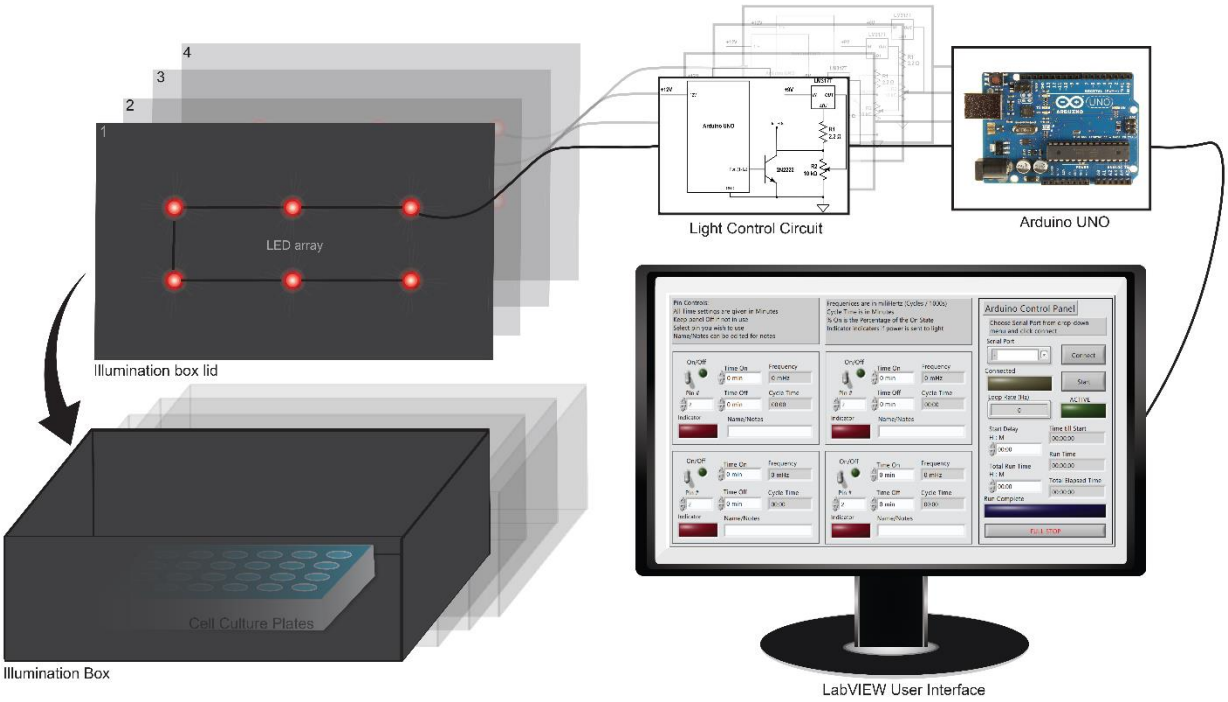

Figure S5: Illumination setup consists of black boxes with LED arrays controlled via an Arduino-driven circuitry and a LabVIEW user interface. The system is easily expandable to allow for the control of up to 12 boxes simultaneously. Each box can be activated at different time intervals and at different frequencies.

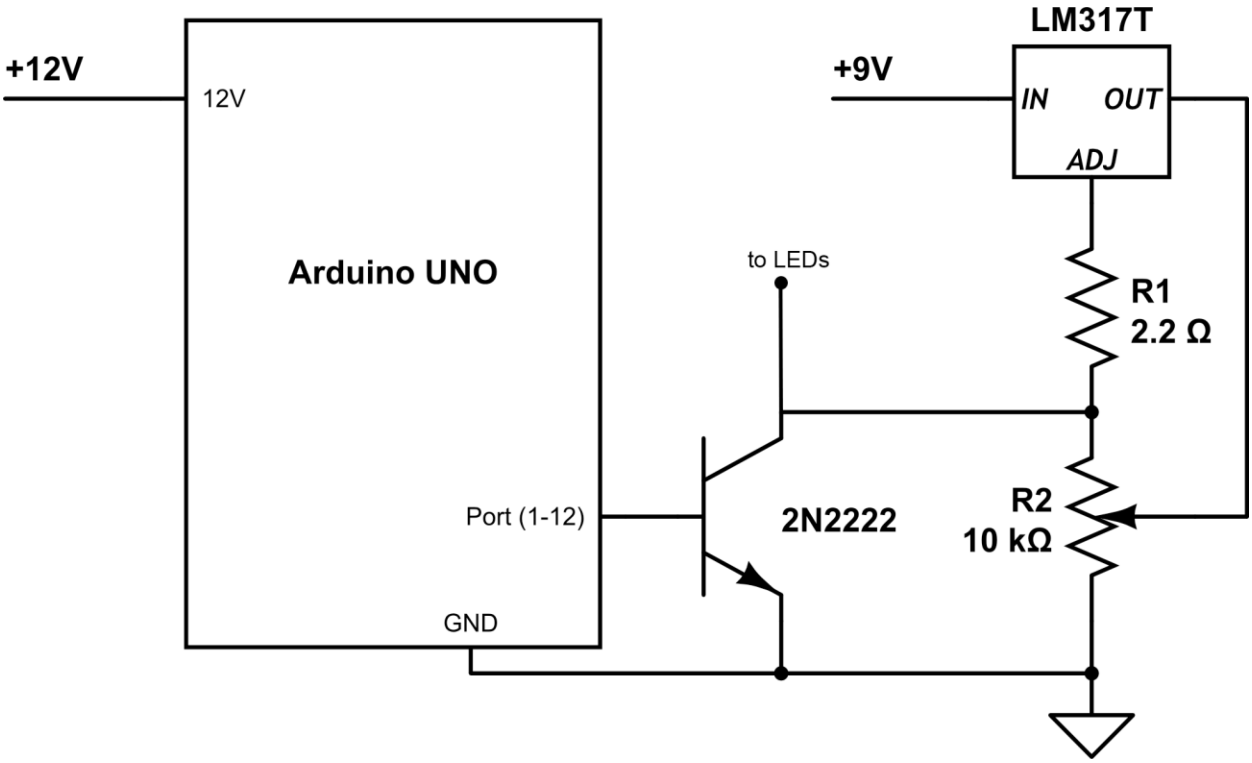

Figure S6: Circuit Design for LED illumination. Electronic schematic of the circuit used to control the LEDs for each box, coupled with an Arduino UNO. The circuit requires a 9 Volt voltage source and uses simple components. A trimmer potential allows for intensity and brightness control of the LEDs. This circuit can control 6 high power LEDs in series.

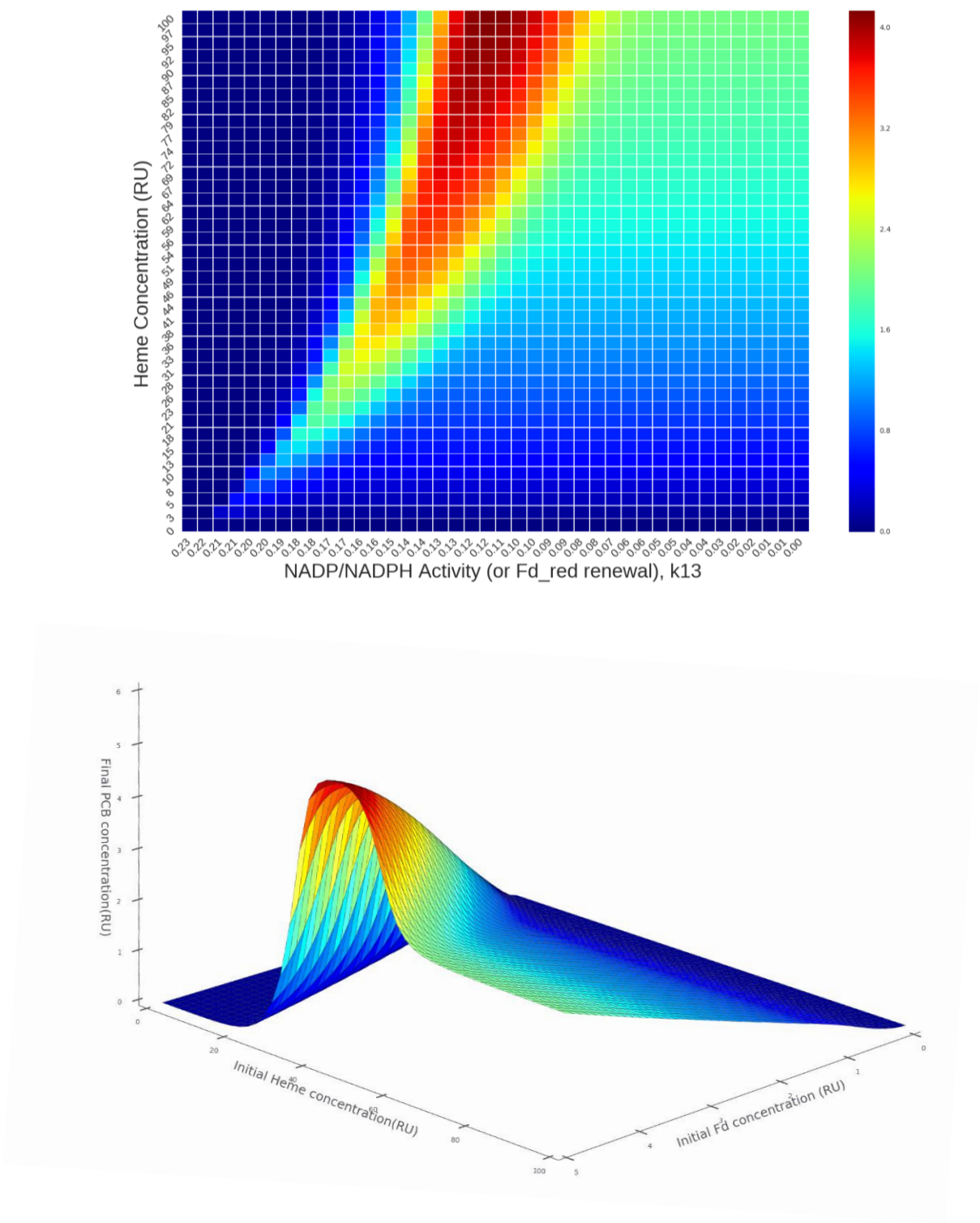

Figure S7: Kinetic model results. By varying the initial Heme concentrations and the rate of renewal of Fd_{oxi} to Fd_{red}, we show the dependence on these parameters in the PCB pathway.

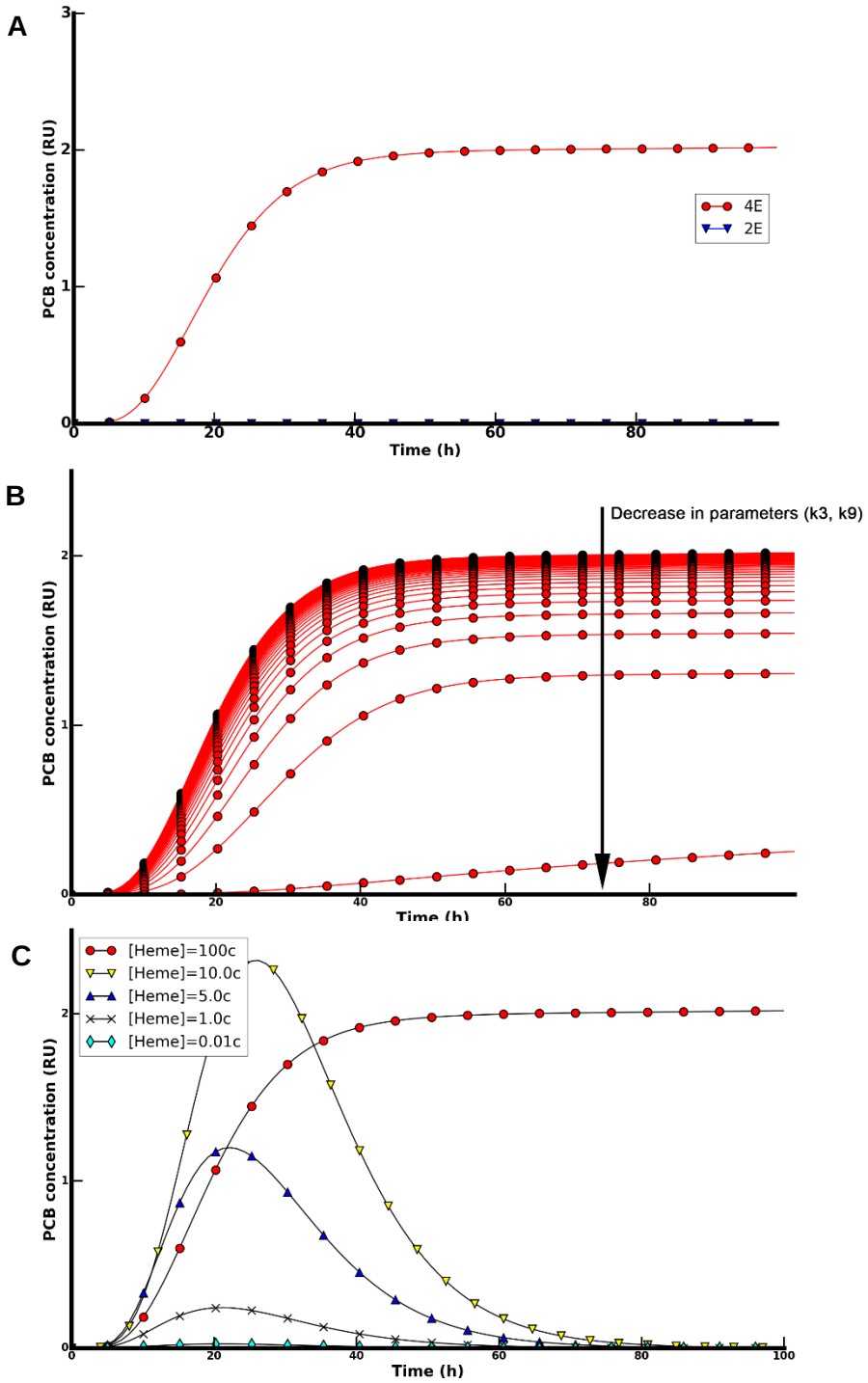

Figure S8: Kinetic model results. **(A)** We simulate the presence and absence of the FD: FNR complex, demonstrating more robust production of PCB with the 4 enzymes. **(B)** Decreasing sweep through the parameters k_3 and k_9, which control binding of HO1 and PcyA to Fd respectively. This graph shows that

with decreasing species specificity, a decrease in PCB production is observed. **(C)** Varying initial concentrations of heme, demonstrating PCB dependence to Heme levels.

Supplementary Note. Model codes and Illumination user Interface.

1. Full working model (in python 2.7), plus scripts to generate Supplementary Figures S7 and S8. In order to execute the code, it is necessary to install the python package PySB (http://pysb.org/) and dependencies. All files should be placed in the same folder for execution.

2. LabVIEW Visual Interface Note that this requires a working LabVIEW installation in your computer. If you need an executable (.exe) file, please contact the article's corresponding authors.

File:

Kyriakakis_et_al_LabView_Software.vi

References:

(1) Lopez, C. F., Muhlich, J. L., Bachman, J. A., and Sorger, P. K. (2013) Programming biological models in Python using PySB. *Mol Syst Biol 9*, 646.

(2) Tu, S. L., Gunn, A., Toney, M. D., Britt, R. D., and Lagarias, J. C. (2004) Biliverdin reduction by cyanobacterial phycocyanobilin:ferredoxin oxidoreductase (PcyA) proceeds via linear tetrapyrrole radical intermediates. *J Am Chem Soc 126*, 8682–8693.

(3) Batie, C. J., and Kamin, H. (1984) Electron transfer by ferredoxin:NADP+ reductase. Rapid-reaction evidence for participation of a ternary complex. *J Biol Chem 259*, 11976–11985.

(4) Hanke, G. T., Kurisu, G., Kusunoki, M., and Hase, T. (2004) Fd : FNR Electron Transfer Complexes: Evolutionary Refinement of Structural Interactions. *Photosyn Res 81*, 317–327.

(5) Hanke, G., and Mulo, P. (2013) Plant type ferredoxins and ferredoxin-dependent metabolism. *Plant Cell Environ 36*, 1071–1084.

(6) Okada, K. (2009) HO1 and PcyA proteins involved in phycobilin biosynthesis form a 1:2 complex with ferredoxin-1 required for photosynthesis. *FEBS Lett 583*, 1251–1256.

(7) Frankenberg, N., and Lagarias, J. C. (2003) Phycocyanobilin:ferredoxin oxidoreductase of Anabaena sp. PCC 7120. Biochemical and spectroscopic. *J Biol Chem 278*, 9219–9226.

(8) Müller, K., Engesser, R., Timmer, J., Nagy, F., Zurbriggen, M. D., and Weber, W. (2013) Synthesis of phycocyanobilin in mammalian cells. *Chem Commun (Camb) 49*, 8970–8972.

(9) Chellaboina, V., Bhat, S., Haddad, W., and Bernstein, D. (2009) Modeling and analysis of mass-action kinetics. *IEEE Control Systems Magazine 29*, 60–78.

(10) Peifer, M., and Timmer, J. (2007) Parameter estimation in ordinary differential equations for biochemical processes using the method of multiple shooting. *IET Syst Biol 1*, 78–88.